INTERLABORATORY COMPARISON OF METHODOLOGIES FOR MEASURING THE ANGLE OF INCIDENCE DEPENDENCE OF SOLAR CELLS

Nicholas Riedel[1], Adrián A. Santamaría Lancia[1], Mekbib Amdemeskel[1], Sune Thorsteinsson[1], Peter B. Poulsen[1], Fabian Plag[2], Ingo Kröger[2], Lenneke H. Slooff[3], Mark J. Jansen[3], Anna J. Carr[3], Petra Manshanden[3], Martin Bliss[4], Tom Betts[4], Iñigo Petrina Jauregui[5], Mikel Ezquer Mayo[5], Jose L. Balenzategui[6], Ruben Roldan[7], Ulli Kräling[8], Ghassan Baarah[8], Beniamino Iandolo[9], Rasmus S. Davidsen[9], Anders Thorseth[1], Carsten Dam-Hansen[1], Gisele A. dos Reis Benatto[1]

[1]Department of Photonics Engineering, Technical University of Denmark, Frederiksborgvej 399, 4000, Roskilde, Denmark
[2]Physikalisch Technische Bundesanstalt (PTB), Bundesallee 100, D-38116 Braunschweig, Germany
[3]Energy Research Centre of the Netherlands (ECN>TNO), P.O. Box 1, 1755 ZG Petten, The Netherlands
[4]Centre for Renewable Energy Systems Technology (CREST), Loughborough University, Loughborough, Leicestershire, LE11 3TU, UK
[5]Spanish National Renewable Energy Centre (CENER), C/Ciudad de la Innovación 7, 31621 Sarriguren (Navarra), Spain
[6]CIEMAT, Department of Energy, Avda. Complutense 40, 28040 Madrid, Spain
[7]University of Applied Sciences and Arts of Southern Switzerland, Institute for Applied Sustainability to the Built Environment (SUPSI - ISAAC), Campus Trevano, CH-6952 Canobbio, Switzerland
[8]Fraunhofer Institute for Solar Energy Systems ISE, CalLab PV Modules, Heidenhofstrasse 2, 79110 Freiburg, Germany
[9]Department of Micro- and Nanotechnology, Technical University of Denmark, Ørsteds Pl., 2800 Kongens Lyngby, Denmark

ABSTRACT — The aim of this work is to compare angle of incidence (AOI) measurement setups for solar cells between laboratories with such capability. For the first time, we compare relative light transmission measurements among eight laboratories, whose measurement techniques include indoor and outdoor methods. We present the relative transmission measurements on three 156 mm x 156 mm crystalline-Si (c-Si) samples with different surface textures. The measurements are compared using the expanded uncertainties provided by each laboratory. Five of the eight labs showed an agreement better than ±2% to the weighted mean between AOIs from -75° to 70°. At AOIs of ±80° and ±85°, the same five labs showed a worst case deviation to the weighted mean of -3% to 5% and 0% to 18%, respectively. When measurement uncertainty is considered, the results show that measurements at the highest incidence angle of ±85° are problematic, as measurements from four out of the six labs reporting uncertainty were found non-comparable within their stated uncertainties. At 85° AOI a high to low range of up to 75% was observed between all eight laboratories.

1 INTRODUCTION

Intercomparisons between laboratories are important to ensure reliable and accurate measurements to the highest level of confidence. Laboratories have different methods, equipment setups and procedures, and it is of great value to assess the comparability of their results. Moreover, the IEC 61853-2 standard, which provides procedures on how to conduct AOI measurements on PV devices was recently published [1]. Thus, a round-robin on AOI measurements will allow us to validate the newly adopted standard, provide feedback to standardization bodies, and establish a baseline that future round-robin campaigns can improve upon. The results from this intercomparison will provide data which will be used in a future study to investigate the impact of measurement deviation on modelling and energy prediction.

The core objective of this work is to determine the level of agreement in the relative transmissivity measurements performed at eight laboratories for each angle of incidence θ. The relative transmissivity is commonly referred to in other works as the incidence angle modifier (IAM). The range of angles extends from -85° to +85° in steps of 5°. The results are analyzed using the E_n number statistical method as outlined in ISO 17043:2010 [2]. This approach is commonly used in proficiency testing and it provides insight to the equivalence of the participating laboratories' test results. The data obtained from the participating laboratories is analyzed with the following objectives: (i) evaluate whether the measurement deviations from the weighted mean are within each partner laboratory's stated uncertainties; (ii) validate if the procedures stipulated by the existing IEC 61853-2 result in comparable measurements when different measurement techniques are used; and (iii) determine the main sources of uncertainty that contribute to non-agreement of measured values between partners.

Although numerous round-robin programs have been conducted for PV measurements at Standard Test Conditions (STC) [3-5], the literature shows comparatively few works on round-robins or laboratory comparisons of angular dependent measurements. The intercomparisons of AOI measurements to date have compared a limited number of laboratories and methods. For example, the authors in [6] compared outdoor measurements performed in real-time at Sandia National Laboratories (SNL) and CFV Solar Test Lab, which lay roughly 10 km apart from each other. These two labs used unique methods to measure the AOI response of full-sized PV modules and found an acceptable level of agreement between their measurements. The authors in [7] compared AOI measurements again performed at SNL on full-sized PV modules to the IAM data for the same modules in PVsyst's database, or to measurements performed at an unnamed third party lab. The authors found that these three sources often had significant deviations for the same module type, up to a 14% difference in relative transmissivity at large AOIs. In this work, we present the AOI measurements made on three unique single cell (156 x 156 mm) laminates by eight European laboratories. The measurement systems encompass five different light sources including one lab that performed the measurements outdoors.

TABLE I: Description of participating laboratory measurement systems [8-11].

Laboratory	Test condition	Rotation stage	Description of light source
CENER	Outdoor	1-axis, 0° to 90°, Automated	Natural sunlight. Diffuse directly measured
CIEMAT	Indoor	1-axis, +90° to -90°, Automated	Continuous collimated broadband halogen lamp (1kW DXW)
CREST	Indoor	1-axis, +90° to -90°, Automated	Pasan 3b flasher with broadband Xe arc lamp (class AAA)
DTU	Indoor	1-axis, +90° to -90°, Automated	Energetiq (EQ-99FCX) broadband laser driven light source
ECN>TNO	Indoor	1-axis, +90° to -90°, Manual	Pasan flasher with broadband Xe arc lamp (class AAA)
Fraunhofer ISE	Indoor	1-axis, +90° to -90°, Manual	Pasan flasher with broadband Xe arc lamp (class AAA)
PTB	Indoor	2-axis, +90° to -90°, Automated	Tuneable laser system with broadband bias lamps
SUPSI	Indoor	1-axis, +90° to -90°, Automated	Pasan flasher with broadband Xe arc lamp (class AAA)

2 EXPERIMENTAL DETAILS

2.1 *Partner laboratories and procedures*

Eight scientific institutions from six European countries are involved in the measurement comparison. These include the Department of Photonics Engineering at the Technical University of Denmark (DTU Fotonik), Physikalisch Technische Bundesanstalt (PTB), the Energy Research Centre of the Netherlands (ECN>TNO), the Centre for Renewable Energy Systems Technology (CREST) at Loughborough University, the Spanish National Renewable Energy Centre (CENER), the Laboratory of Photovoltaic Solar Energy PVLab at CIEMAT, the University of Applied Sciences and Arts of Southern Switzerland (SUPSI), and Fraunhofer Institute for Solar Energy Systems (ISE). A brief description of each laboratory's measurement setup is described in Table I [8-11].

The measurement systems used at CREST, ECN>TNO, Fraunhofer ISE and SUPSI are based on a flash system used for full-sized modules. However, each one of these labs used a different approach to build the rotation stage. The rotation stage at ECN>TNO, for example is only capable of holding small laminates (roughly 20 x 20 cm), while the CREST, Fraunhofer ISE, and SUPSI rotation stages can accommodate small laminates up to full-sized modules. The CIEMAT and DTU systems are only capable of testing single cell laminates and the PTB system can accommodate mini-modules with up to four 156 x 156 mm cells. DTU was the only laboratory that performed the test with a light source that did not cover the full active cell area (i.e. the diameter of the collimated light beam in the DTU system was 12 mm). The two-axis tracker at CENER can accommodate full-sized module and since single cell laminates were used as the devices under test (DUTs) in this round-robin, they utilized the tracker's area to perform the test on all DUTs at once.

All the participant laboratories were asked to use their standard techniques for AOI measurements. The axis of rotation was predefined in order to allow the results from the different partners to be directly comparable. The definition for which angular direction was positive and negative was made explicitly clear in a memorandum document that all partners received. The document also specified the location of the rotational axis and tolerances for the precise location of the front of the PV cell surface within the laminate. The samples made for this round-robin have an offset of approximately 1.5 mm ±0.5 mm from the rear side (back sheet) to the front surface of the PV cell. The participant laboratories were encouraged to use this tolerance when mounting the samples in their measurement system, although larger deviations from the rotational axis to the center of the PV cell would be acceptable for the outdoor measurement system.

The physical quantity measured by the partner labs is the short circuit current (I_{SC}) of each DUT over the specified angular range. The data of ultimate interest, however, are the relative transmissivity $\tau(\theta)$ values. The relative transmissivity $\tau(\theta)$ - sometimes referred to as the IAM - represents the percentage of in-plane direct beam irradiance available to the PV cell for conversion to electricity. The $\tau(\theta)$ is calculated by normalizing the I_{SC} measured at each angle to the I_{SC} value measured at normal incidence. No procedures were provided to the partner labs as to how to correct for fluctuations in the test environment during the measurement (e.g. spectrum, irradiance or temperature) and instead it was left up to each partner to use their standard correction approach. A common temperature coefficient for I_{SC} was provided to the partner labs in the case temperature corrections were necessary.

2.2 *Devices under test (DUT)*

The round-robin includes measurements of three different PV devices in duplicate (i.e. each lab measures six DUTs in the total). Redundant samples were used so there would always be a backup in the case that any one sample became damaged. Electroluminescence (EL) images were taken before each laboratory started testing to ensure that no damage occurred during transportation. The analysis of EL images taken before the first lab's measurement and after the final lab's measurement showed that no cell damage had occurred during transportation. However, the glass of one sample was damaged about halfway through the campaign, which highlights the necessity of duplicate samples in round-robin campaigns. The measurements made on the damaged sample are not published here.

All DUTs have the following specifications: (i) An active cell area of 156 mm x 156 mm; (ii) full area dimensions of 200 mm x 200 mm; (iii) 3.2 mm thick finely textured PV glass superstrate; (iv) ethylene-vinyl acetate (EVA) encapsulant; (v) two tabs as metal contacts; and (vi) a flat polymeric backsheet with slight curvature around the cell edges. The differences between the DUTs are the cell types and cell texturing. Two DUTs are mono-crystalline standard silicon; two DUTs are multi-crystalline black silicon textured under reactive ion etch (RIE) treatment (referred to as 'Black-Si A' hereafter) [12]; and two DUTs are multi-crystalline black silicon textured under atmospheric pressure dry etching (ADE) treatment (referred to as 'Black-Si B' hereafter) [13]. The edges of samples were covered with non-transparent tape to prevent measurement artifacts at large incident angles.

IEC 61853-2 specifies that three measurements shall be taken at each angle. Six DUTs and 38 angles per sample would mean that each laboratory needs perform 684 measurements. In most cases, this was not possible due to time constraints and therefore only one measurement per angle, per sample was provided by most laboratories.

2.3 *Uncertainty and Analysis of Results*

Six of the eight labs provided the expanded uncertainty (k = 2) for the value of relative transmissivity $\tau(\theta)$ at each measured angle θ. Two of these labs provided DUT specific uncertainty while the other four provided an uncertainty estimate that covered all samples in this round-robin.

The uncertainty of each lab's measurement is critical for establishing comparability through the E_n number calculation (1). The two labs that were not able to provide measurement uncertainty were assumed to have the worst case uncertainty. That is for every angle measured, the highest uncertainty submitted by any lab is used as the measurement uncertainty for the labs without uncertainty.

For every sample and every angle, an E_n number is calculated per (1).

$$E_n = \frac{x_i - X_{ref,i}}{\sqrt{UC_i^2 + UC_{ref,i}^2}} \qquad (1)$$

Wherein x_i is the individual laboratory's measured relative transmissivity $\tau(\theta)$ and UC_i is the expanded (k = 2) uncertainty of the lab's measurement of $\tau(\theta)$. The reference value $X_{ref,i}$ is the weighted mean of all partner´s measured $\tau(\theta)$ values for a given sample at a given angle. Here the measurements are weighted by the uncertainty provided by each partner. Weighting the results in this manner has the consequence of shifting the X_{ref} value towards the measured values (x_i) of the laboratories with lower uncertainty. For every sample and every angle, the $X_{ref,i}$ value is calculated using equation (2).

$$X_{ref,i} = \frac{\sum_{i=1}^{N} \frac{x_i}{\sigma_i^2}}{\sum_{i=1}^{N} \frac{1}{\sigma_i^2}} \qquad (2)$$

Wherein σ_i is the k = 1 uncertainty of the lab's measurement. The value σ_i is squared in (2) to arrive at the variance, which is additive by nature, whereas the standard deviation is not. Finally, $UC_{ref,i}$ is the expanded (k = 2) combined uncertainty of $X_{ref,i}$ and is calculated per (3). Calculating UC_{ref} in this way yields a value that is always lower than any of the participating labs' declared uncertainties.

$$UC_{ref,i} = \frac{2}{\sqrt{\sum_{i=1}^{N} \frac{1}{\sigma_i^2}}} \qquad (3)$$

The relative transmission measurements from each laboratory are said to be coherently within their declared uncertainty when -1 ≤ E_n ≤ 1. In other words, the condition -1 ≤ E_n ≤ 1 is met when the difference between a lab's measurement (x_i) and the reference value ($X_{ref,i}$) is less than or equal to the root sum of squares (RSS) of the lab's declared uncertainty (UC_i) and the reference uncertainty ($UC_{ref,i}$). The sign of E_n provides a convenient way of discerning whether a lab's measurement is high (E_n = +) or low (E_n = -) relative to the weighted group mean.

3 RESULTS

The expanded uncertainty provided from each partner laboratory is shown as a function of AOI in Figure 1. Since there were three unique DUTs in the campaign, some labs accordingly reported an expanded uncertainty for each of the three DUTs. The uncertainty from partners who did provide DUT specific uncertainty (CREST and PTB) is represented by range bars and a dot symbol. The range bars show the maximum and minimum uncertainty reported by the laboratory while the dot in the middle represents their median uncertainty. The same convention is used to represent UC_{ref}. Note how UC_{ref} is less than the uncertainty of all laboratories at each angle. The uncertainty provided by partners with non-DUT specific uncertainty is represented with 'x' symbols. Figure 1 shows a trend of increasing uncertainty with increasing AOI, wherein a range of 0.1% to 3% at normal incidence and a range of 2.5% to 9.3% at 85° AOI is observed. The specific reasons for this increasing trend will be unique to a given measurement system (e.g. increasing non-uniformity or uncertainty of the measured angle θ). In the DTU measurement system, for example, the increase of uncertainty at large angles is primarily due to an increased contribution of uncertainty from the measured angle θ.

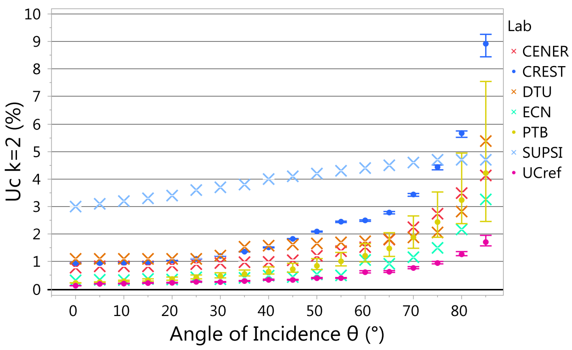

Figure 1: Expanded uncertainty from six laboratories as a function of AOI. The expanded uncertainty of the reference (UC_{ref}) is also shown. Labs providing a single uncertainty value at each angle are noted with an 'x' whereas labs with uncertainty specific to each DUT are noted with dots and range bars.

The measurements on sample Black-Si A performed by the eight partner laboratories are shown in Figure 2. We show the high-level results from this sample only because the measurement differences between the labs showed a consistent trend and because sample Black-Si A showed the worst case range (max-min) among the eight labs. Figure 2 shows an increasing measurement range between the labs with an increasing AOI. This result follows the same trend of increasing uncertainty with increasing AOI purported by the partner laboratories. In the positive direction, the measurement range is less than 0.1 (10%) up to a +60° AOI, while in the negative direction the range is less than 0.1 up to a -70° AOI. We attribute the difference between measurements at positive and negative angles to an artifact in some participant's results, not because of an inherent non-symmetry in the DUT itself. The maximum disagreement of 0.69 (69%) and 0.75 (75%) is observed at +85° and -85° AOI, respectively. This large disagreement is mostly driven by the outdoor measurement performed by CENER. If this measurement is removed, the range at 85° AOI is decreased to 0.23 (23%) in the positive direction and 0.36 (36%) in the negative direction.

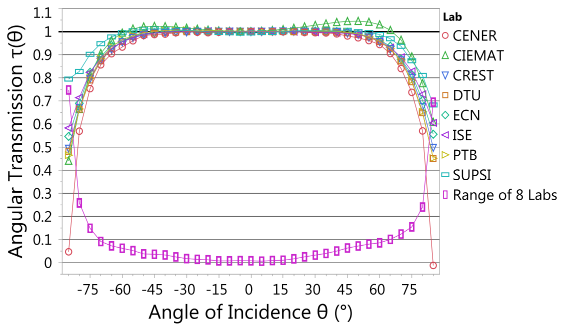

Figure 2: Overlay of transmission as a function of AOI θ as measured by eight laboratories on sample Black-Si A. The range of all measurements is also shown.

In Figure 3 we show the difference between each lab's angular transmission measurement $\tau(\theta)$ and the reference value X_{ref}. Recall that there are three DUTs, and thus three X_{ref} values at each AOI. The error bars drawn around each data point represent the maximum and minimum difference to the reference value; the center of the data point between the bars represents the median difference. Note that the deltas of -33% to -45% at ±85° reported by CENER have been removed from the plot in order to create a finer view of the y-axis.

Figure 3 shows that the agreement between all labs relative to the weighted mean is better than ±2% in the limited range of AOIs from -30° to 25°. However, it is only the measurements from CIEMAT and SUPSI that show dispersion from the group at low angles. If CIEMAT and SUPSI's data are excluded, then the agreement between the six remaining labs is better than ±2% for AOIs -50° to 50°. Beyond -50° to 50°, CENER's measurements become increasingly lower relative to the other labs'. If CENER's measurements are also excluded, five of the eight labs have an agreement of better than ±2% from the weighted mean on all samples between -75° to 70°. At ±80° these same five labs show worst case agreement of -3% to 5% relative to the weighted mean (Black-Si A), and a best case agreement of -1% to 0.5% relative to the weighted mean (Mono-Si). And finally, at ±85° the five labs show worst case agreement of 0% to 18% relative to the weighted mean (Black-Si B) and a best case agreement of 0.5% to 8.5% (Mono-Si). The worse agreement on the Black-Si as compared to Mono-Si sample could be due to the difference in surface structures or differences in low-light behavior.

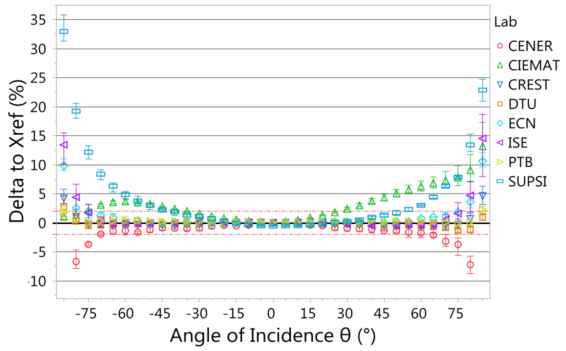

Figure 3: Plot showing the difference between each lab's measurement and the reference value X_{ref}. The error bars show each lab's max and min difference to X_{ref}. The red dashed reference lines are drawn at ±2%.

In Figure 4 we present the results from the E_n number calculation as a function of AOI for the Black-Si A sample. The profile observed in Figure 4 is similar to that in Figure 3 because the data in Figure 3 are the numerator used in the E_n calculation. Figure 4 shows 39 (of 280 total) measurements where the results are not comparable within the stated or assumed uncertainties. In other words, 14% of the time E_n is greater than 1 or less than -1, wherein all instances occur at AOIs ≥ |±40|°. PTB and CREST are the only two labs whose measurements result is $-1 \leq E_n \leq 1$ for all AOIs. Thus, we can say that their measurements agree to the weighted mean within the stated uncertainties for all measurement angles.

The CIEMAT data show 10 instances of non-comparability. Therefore the worst case uncertainty assumed for the CIEMAT measurements is clearly too conservative to make them comparable to the rest of the partners. Interestingly, CIEMAT shows several instances of non-comparability in the positive angular direction, but none in the negative direction. This is due to the non-symmetrical measurements they obtained (Figure 2). The reason behind the non-symmetry is still uncertain, but we believe it is likely due to an offset in the vertical axis of rotation from the middle of the PV cell. In addition, it is also possible that the optics unique to the CIEMAT measurement system result in the partial polarization of light from the halogen lamp, which in return would alter the reflection and transmission properties.

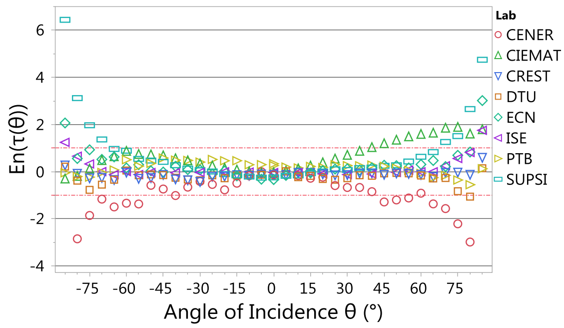

Figure 4: E_n number as a function of AOI θ for the measurements from eight laboratories.

The CENER data show 16 instances of measurements that deviate from the weighted mean beyond their reported uncertainty level. The CENER measurements are consistently lower than the measurements from the other seven partners and this difference increases at higher AOIs. The CENER measurements were the only measurements in this round-robin performed outdoors. However, we do not conclude that the low results are attributable to the outdoor approach itself. To better understand the differences that can occur indoors versus outdoors, we propose to extend the measurement campaign to additional laboratories performing the AOI test outdoors.

The SUPSI data show 8 instances where their measurements do not agree within the stated uncertainty and all 8 instances occur at AOIs ≥ |±70|°. Although the SUPSI measurements are consistently higher than most of the labs at every AOI (Figure 2 and Figure 3), they are also the lab with the most conservative uncertainty. However, the stated uncertainty of 4.6% to 4.7% at AOI ≥ 70° is not conservative enough for comparability. The reason(s) for SUPSI's higher than average angular transmission measurements are still under investigation. At the time of writing the high measurements are believed to be due to unwanted reflections within the test bed. These reflections are more pronounced in the negative direction than in the positive direction. The SUPSI data show that establishing comparability is not dependent on the light source used. CREST, ECN>TNO, ISE and SUPSI all used Xe flash lamps to measure the samples and yet SUPSI shows significant deviations from the other three labs.

DTU, ECN>TNO and ISE all show generally good agreement to the weighted mean; each lab shows one or two instances where their measurements are not comparable within the stated or assumed uncertainties. For DTU this occurs at AOI of 80° while for ECN>TNO and ISE it occurs at the extreme angles of ±85°. In actuality the measurements from ECN>TNO are closer to the weighted mean than ISE's at these high AOIs, since the uncertainties provided by ECN>TNO are more conservative than the maximum uncertainty assigned to the ISE measurements.

To understand the uncertainty level necessary for CIEMAT and ISE to be comparable to the weighted mean, we solve (1) for UC_i while leaving $E_n = 1$ and $X_{ref,i}$ and $UC_{ref,i}$ constant based on results from the other six labs. The results are shown in Figure 5 for the Black-Si A sample. The maximum uncertainty at each AOI reported by any of the other six labs is also shown. Since the expanded uncertainty limit for ISE is less than 1% out to ±65°, we can conclude that their measurements agree well to the weighted mean within that range. However, an uncertainty between 11.7% and 17.7% at the highest angles of ±85° would be required for comparability.

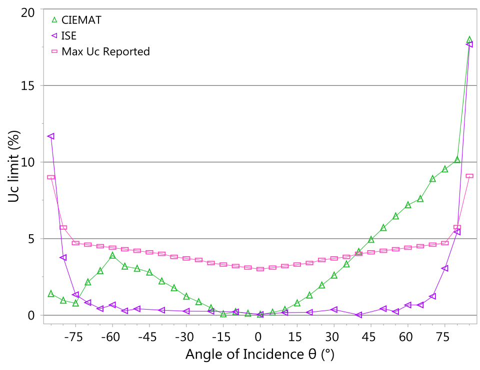

Figure 5: Minimum uncertainties required in order for CIEMAT's and ISE's measurements to be comparable to the weighted mean of the other six labs.

As mentioned, the measurement differences between labs showed the same trend across all three samples. Nevertheless we wish to give a full perspective of how the E_n number varied across samples and angles. In Figure 6, we show the number of labs that had an E_n number outside the limit of comparability. Figure 6 shows that at the extreme AOIs half or more of the labs have deviations that are not fully covered by their uncertainty budgets. This result highlights the difficulty of performing accurate measurements at high AOIs. Figure 6 includes all eight laboratories and assumes the worst case uncertainty for the ISE and CIEMAT data.

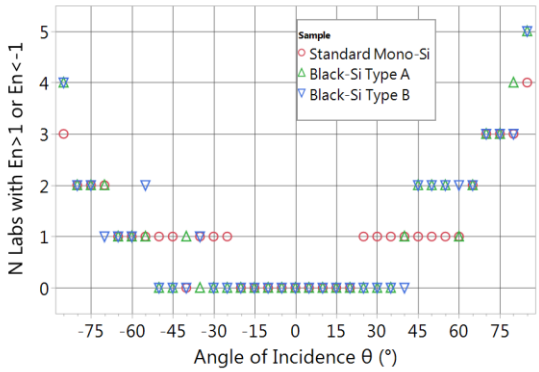

Figure 6: Plot showing the number of labs that do not comply to the condition $-1 \leq E_n \leq 1$ as a function of AOI.

IEC 61853-2 states that the rotational symmetry of the test system shall be verified at -80° and 80° AOI. It further states that the deviation in the relative transmissivity at these two angles shall not deviate by more than 2%. We performed this check for all eight laboratories and the results for the Black-Si A sample are shown in Figure 7. The limits of ±2% are indicated by the dashed red reference lines. It can be seen in Figure 7 that the labs who were the most comparable always meet the IEC requirement for symmetry. On the contrary, the labs with the lowest comparability and largest deviations from the weighted mean, showed symmetry that did not comply with the standard. This result suggests that it is a good practice to verify the symmetrical performance of a test system for measurement of the angular dependency of PV devices.

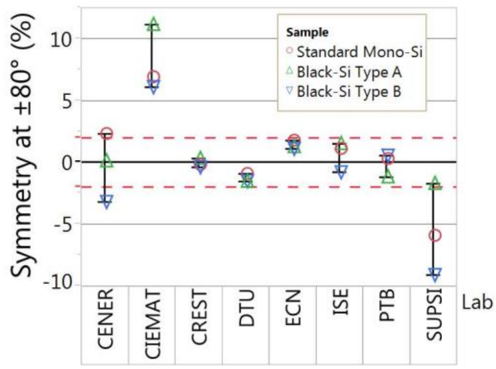

Figure 7: Variability plot showing the symmetry of the relative transmissivity measurements at ±80°. Three data points are shown for each lab, one for each sample.

4 SUMMARY

The results from an international round-robin between eight laboratories performing angular dependent measurements have been presented. Five of the eight labs showed an agreement better than ±2% between AOIs from -75° to 70°. At AOIs of ±80° and ±85°, the same five labs showed a worst case deviation to the weighted mean of -3% to 5% and 0% to 18%, respectively. These worst cases were observed on the 'Black-Si A' and 'Black-Si B' samples. The results showed that measurements at the highest incidence angle of ±85° are problematic, where a high to low range of up to 75% was observed among the eight labs.

The results provided by CREST and PTB agreed to the weighted average within their stated uncertainties for all angles. Similarly, the results from DTU and ECN>TNO agreed to the weighted average within their uncertainties, for all angles except 85°. At high angles of incidence (≥ 70°) the measurements from three to five labs were found not comparable within their stated or assumed uncertainties. The more frequent non-comparability observed at high angles of incidence suggests that labs may need to reconsider a more conservative uncertainty budget at angles ≥ 70°.

In a future work we will investigate the influence of the measurement deviations observed in this round-robin on modelled energy production. Furthermore, we plan to extend the round-robin to obtain more data from laboratories performing the AOI test outdoors.

5 ACKNOWLEDGEMENTS

We would like to thank all the partner laboratories for all their time and work performing the measurements. The facility and part of the work at DTU has been made possible by the grant "LEDMET - Center for LED metrology" from Innovation Fund Denmark.

6 REFERENCES

[1] "IEC 61853-2, Photovoltaic (PV) module performance testing and energy rating - Part 2: Spectral responsivity, incidence angle and module operating temperature measurements." 2016.

[2] "ISO/IEC 17043:2010 Conformity Assessment – General Requirements for Proficiency Testing International Organization for Standardization." 2010

[3] B. Mihaylov *et al.*, "Results of the SOPHIA intercomparison Part-1: STC, low-irradiance conditions and temperature coefficient measurements of C-Si technologies" in *29th Eur. Photovolt. Sol. Energy Conf. Exhib.,2014*

[4] D. Dirnberger *et al.,* "Progress in photovoltaic module calibration: Results of a worldwide intercomparison between four reference laboratories" *Meas. Science and Tech.,* vol. 25. no. 10, 2014.

[5] E. Salis *et al.,* "Improvements in world-wide intercomparison of PV module calibration," *Solar Energy,* Volume 155, October 2017, Pages 1451-1461

[6] B. H. King *et al.,* "Recent advancements in outdoor measurement techniques for angle of incidence effects," in IEEE 42nd *Photovoltaic Specialist Conference (PVSC)*, 2015

[7] S. Boppana *et al.,* "Impact of uncertainty in IAM measurement on energy predictions," *7th World Conference on Photovoltaic Energy Conversion (WCPEC-7) 2018*

[8] M. W. Amdemeskel *et al.*, "Indoor measurement of Angle resolved light absorption by antireflective glass in solar panels", *34th Eur. Photovolt. Sol. Energy Conf. Exhib., 2017*

[9] J.L. Balenzategui and F. Chenlo, "Measurement and analysis of angular response of bare and encapsulated silicon solar cells," *Sol. Energy Materials & Sol. Cells*, vol. 86, pp. 53–83, 2005.

[10] F. Plag , I. Kröger, T. Fey, F. Witt, & S. Winter "Angular-dependent spectral responsivity - Traceable measurements on optical losses in PV devices" *Prog. Photovoltaics Res. Appl.*,Special Issue Paper, pp. 1–14, 2017.

[11] L.H. Sloof *et al.*, "Looking at the annual yield from various angles: Optical model verification for structured glass" in *33rd Eur. Photovolt. Sol. Energy Conf. Exhib., 2016*

[12] R. S. Davidsen *et al.*, "Black silicon laser-doped selective emitter solar cell with 18.1% efficiency," *Sol. Energy Materials & Sol. Cells*, vol. 144, pp. 740–747, 2016.

[13] B. Kafle *et al.*, "Plasma-free dry-chemical Texturing process for high-efficiency multicrystalline silicon solar cells," *Energy Procedia*, vol. 92, no. September, pp. 359–368, 2016.